

Fracture functions from back-to-back dihadron production

Timothy B. Hayward, Harut Avakian, Aram Kotzinian



May 23, 2022

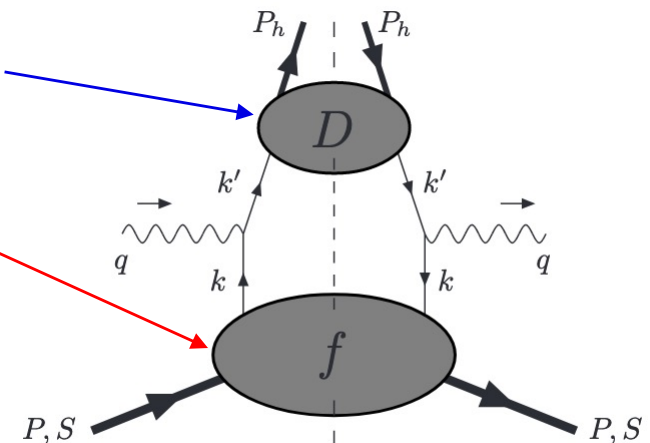
UConn

Traditional SIDIS measurements

- Decades of study have led to detailed mappings of the momentum distribution of partons in the nucleon in terms of 1-D and 3-D (TMD) parton distribution functions (PDFs).
- SIDIS measurements rely on the assumption that measured hadrons are produced in the CFR.
- Cross section factorized as a convolution of PDFs and Fragmentation Functions (FFs)¹.

$$\frac{d\sigma^{\text{CFR}}}{dx_B dy dz_h} = \sum_a e_a^2 f_a(x_B) \frac{d\hat{\sigma}}{dy} D_a(z_h)$$

- PDFs
 - Confined motion of quarks and gluons inside the nucleus
 - Orbital motion of quarks, correlations between quarks and gluons
- Fragmentation Functions
 - Probability for a quark to form particular final state particles
 - Insight into transverse momenta and polarization



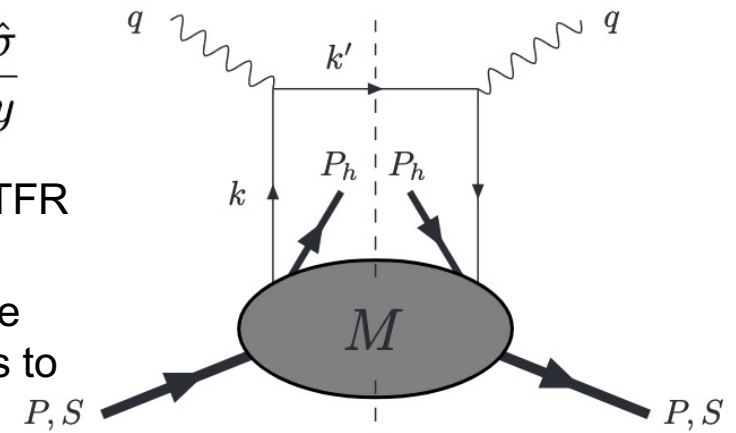
M. Anselmino et al., Phys. Lett. B. 706 (2011), 46-52, [hep-ph] 1109.1132

The Neglected Hemisphere – Target Fragmentation

- Final state hadrons also form from the left-over target remnant (TFR) whose partonic structure is defined by “fracture functions”^{1,2}: the probability for the target remnant to form a certain hadron given a particular ejected quark.
- In the TFR, factorization into x and z does not hold because it is not possible to separate quark emission from hadron production.

$$\frac{d\sigma^{\text{TFR}}}{dx_B dy dz} = \sum_a e_a^2 (1 - x_B) M_a(x_B, (1 - x_B)z) \frac{d\hat{\sigma}}{dy}$$

- Sometimes possible to kinematically separate CFR and TFR ... but not always clear.
- Studying the TFR tests our complete understanding of the SIDIS production mechanism while also providing access to information not available in the CFR.



M. Anselmino et al., Phys. Lett. B. 706 (2011), 46-52, [hep-ph] 1109.1132

Categorizing Fracture Functions

- At leading twist 16 fracture functions exist that can be organized into tables of quark and nucleon polarizations just like the more familiar PDFs.

		Quark polarization		
		U	L	T
Nucleon polarization	U	f_1		h_1^\perp
	L		g_{1L}	h_{1L}^\perp
	T	f_{1T}^\perp	g_{1T}	h_1, h_{1T}^\perp

CFR

 \longleftrightarrow

TFR

		Quark polarization		
		U	L	T
Nucleon polarization	U	\hat{u}_1	$\hat{l}_1^{\perp h}$	$\hat{t}_1^h, \hat{t}_1^\perp$
	L	$\hat{u}_{1L}^{\perp h}$	\hat{l}_{1L}	$\hat{t}_{1L}^h, \hat{t}_{1L}^\perp$
	T	$\hat{u}_{1T}^h, \hat{u}_{1T}^\perp$	$\hat{l}_{1T}^h, \hat{l}_{1T}^\perp$	$\hat{t}_{1T}^h, \hat{t}_{1T}^{\perp h}$ $\hat{t}_{1T}^{\perp\perp}, \hat{t}_{1T}^{\perp h}$

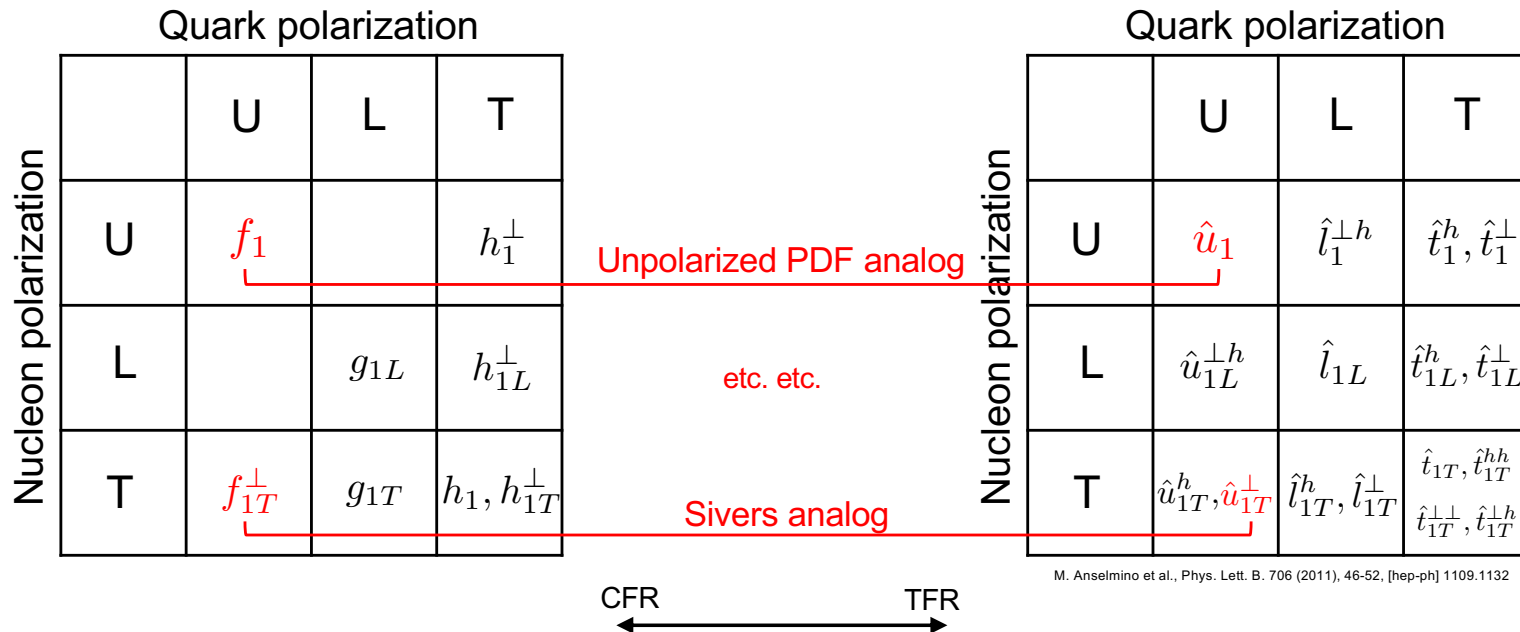
M. Anselmino et al., Phys. Lett. B. 706 (2011), 46-52, [hep-ph] 1109.1132

Analog to PDFs; Momentum Sum Rules

- A direct relationship exists to the eight leading twist PDFs after the fracture functions are integrated over the fractional longitudinal nucleon momentum, ζ .

$$\sum_h \int_0^{1-x} d\zeta \zeta M_a(x, \zeta) = (1-x) f_a(x)$$

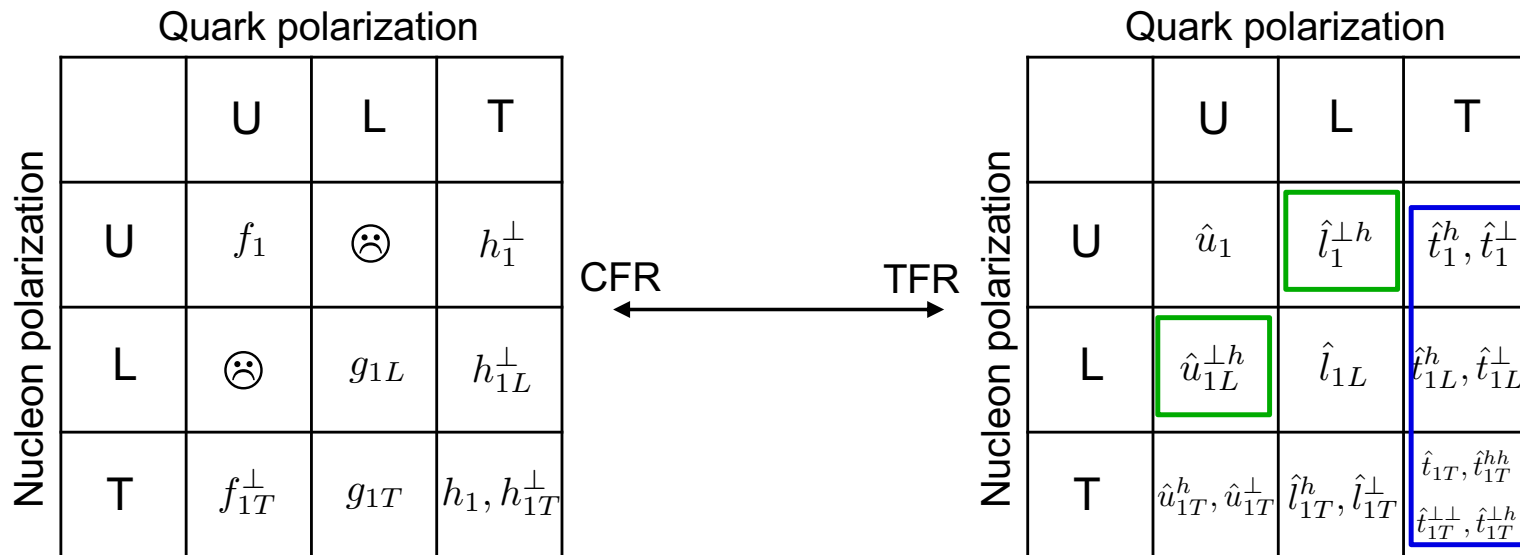
M. Anselmino et al., Phys. Lett. B. 699 (2011), 108, [hep-ph] 1102.4214



M. Anselmino et al., Phys. Lett. B. 706 (2011), 46-52, [hep-ph] 1109.1132

Single hadron limitations

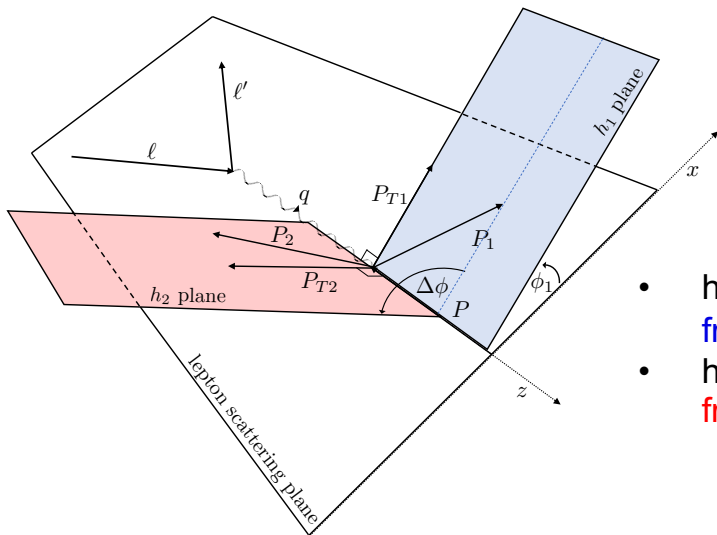
- FrFs describing transversely polarized quarks are chiral odd and inaccessible in single hadron production.
- Functions with double superscripts containing h and \perp have no analog and disappear after integration over either momentum.



M. Anselmino et al., Phys. Lett. B. 706 (2011), 46-52, [hep-ph] 1109.1132

Back-to-back Formalism

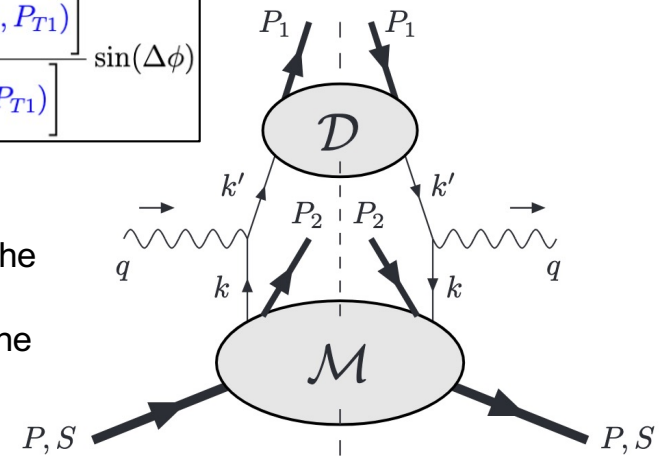
- When two hadrons are produced “back-to-back”^{1,2} with one in the CFR and one in the TFR the structure function contains a convolution of a **fracture function**, $\hat{l}_1^{\perp h}$, and a **fragmentation function**, D_1 .



Kinematic plane for b2b dihadron production.

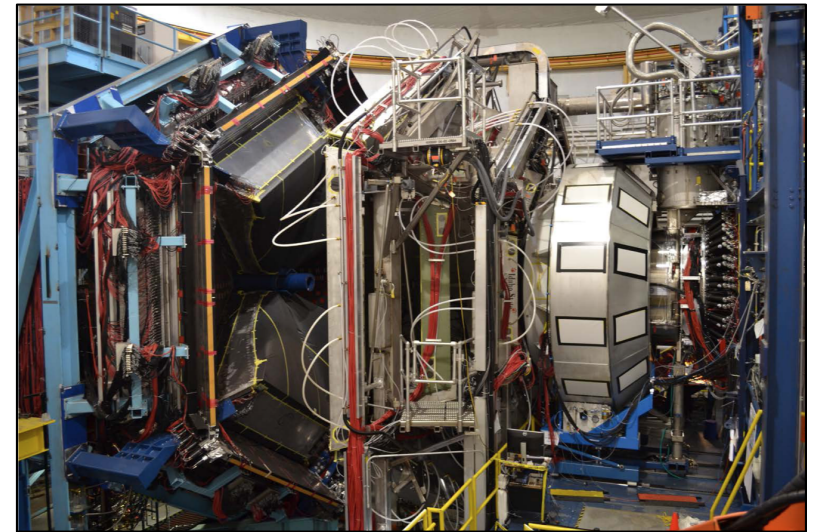
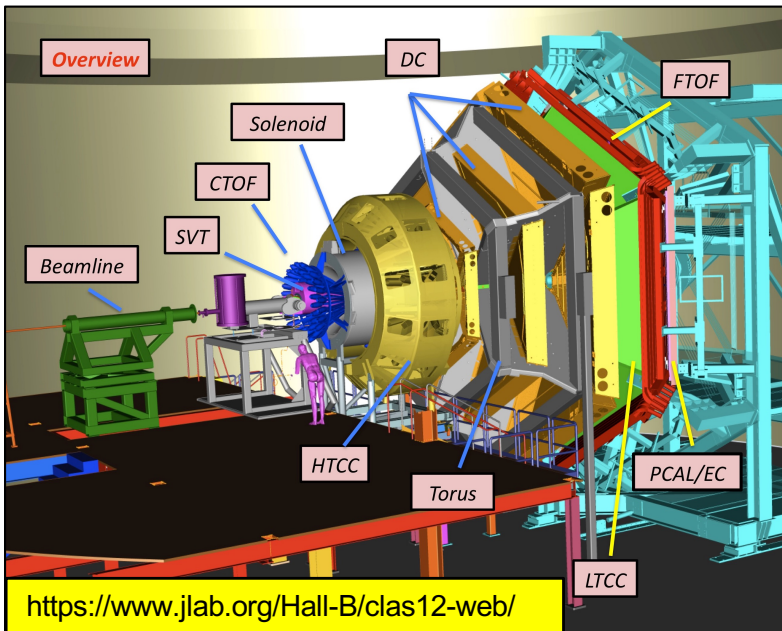
$$A_{LU} = -k(\epsilon) \frac{P_{T1} P_{T2}}{m_1 m_2} \frac{\mathcal{C} \left[w_5 \hat{l}_1^{\perp h}(x, \zeta_2, P_{T2}) D_1(z_1, P_{T1}) \right]}{\mathcal{C} \left[\hat{u}_1(x, \zeta_2, P_{T2}) D_1(z_1, P_{T1}) \right]} \sin(\Delta\phi)$$

- h_1 in the CFR with production dictated by the **fragmentation function**
- h_2 in the TFR with production dictated by the **fracture function**



Handbag diagram for dihadron production; lower blob contains FrFs and upper blob contains the FFs.

CLAS12 Experimental Setup



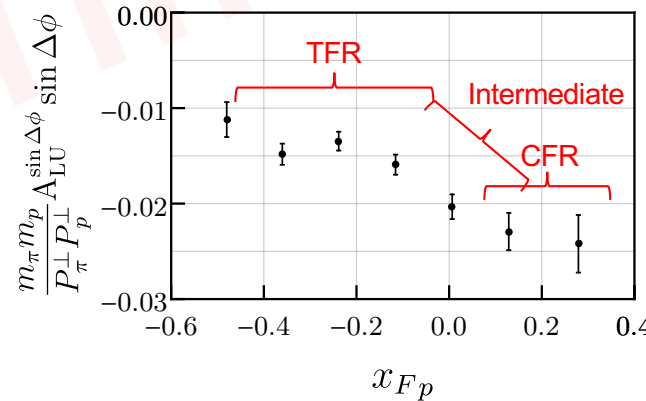
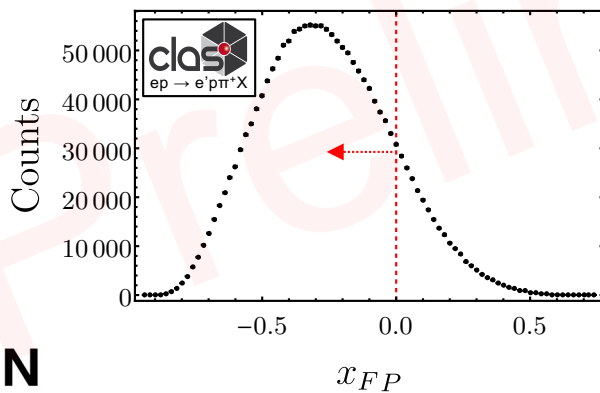
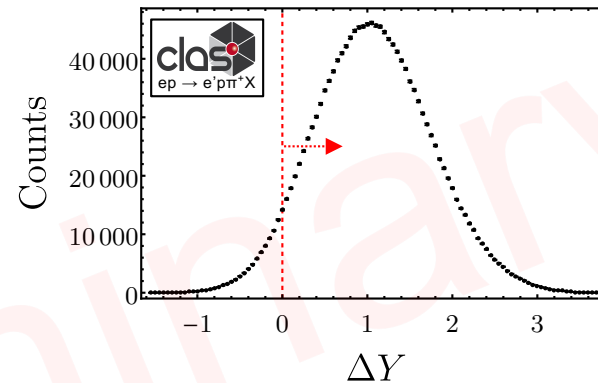
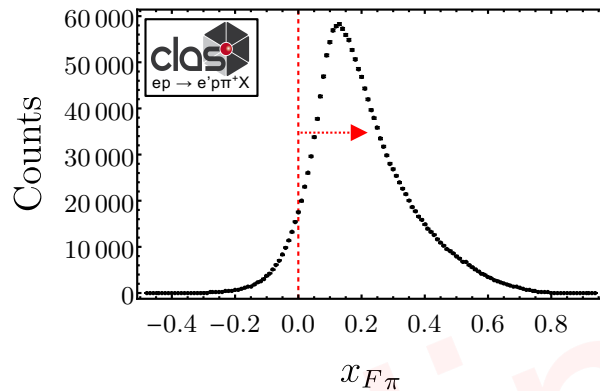
V. Burkert et al., Nucl. Instrum. Meth. A 959 (2020) 163419

- CLAS12: very high luminosity, wide acceptance, low Q^2 (higher twist measurements)
- Began data taking in Spring 2018 – many “run periods” now available.
- 10.6 (2018) and 10.2 (2019) GeV electron beam, longitudinally polarized beam, liquid H₂ target.



Selecting back-to-back events

- A natural choice for a first analysis are events with a pion (CFR biased) and proton (TFR biased).



$$x_F = \frac{2p \cdot q}{|q|W}$$

$$Y = \frac{1}{2} \log \left[\frac{E_h + p_z}{E_h - p_z} \right]$$

Early signs of separate signatures in both interaction regions (see next talk!).

Extracting A_{LU}

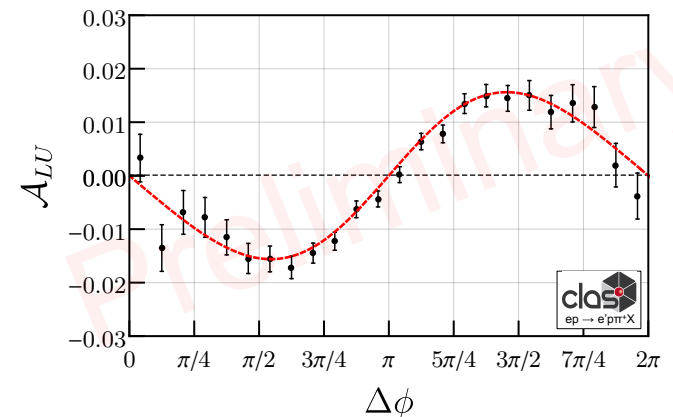
- Select $ep \rightarrow e'P \pi^+ + X$.
- Consider all possible hadron pairs.
- Amplitudes are extracted simultaneously via maximizing a likelihood function.
- Unbinned maximum likelihood method:

$$-\ln \mathcal{L}_{ML}(A) = N - \sum_i^N \ln \left[1 + h_i P_i (A_1 \sin \Delta\phi_i + A_2 \sin 2\Delta\phi_i) \right]$$

- Include relevant beam polarization ($\sim 85\%$ at JLab).

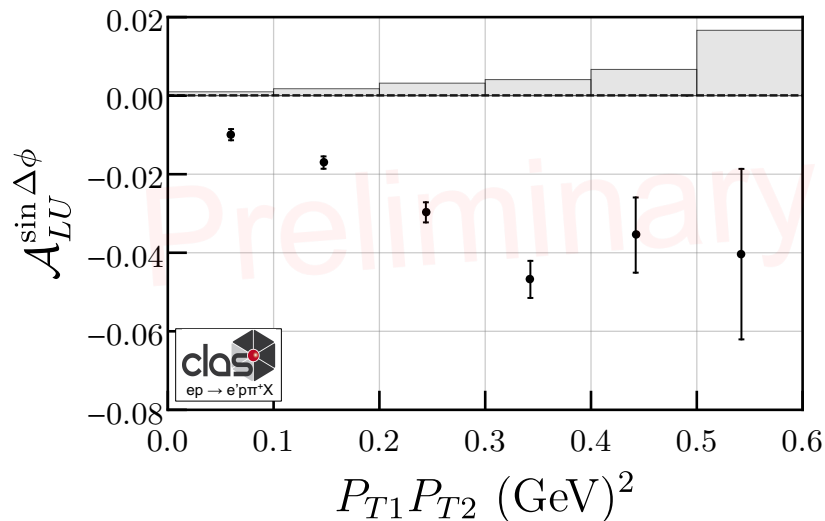
Channel selection

- $Q^2 > 1.0 \text{ GeV}^2$
- $W > 2.0 \text{ GeV}$
- $M_x > 0.90 \text{ GeV}$
- $y < 0.75$
- $\Delta Y > 0$
- $x_{f1} > 0$
- $x_{f2} < 0$
- $Z_1 > 0.2$
- $M_h > 1.5 \text{ GeV}$



Initial Observation

- Observed linear dependence on the product of transverse momenta is consistent with expectations (linear, goes to zero at zero transverse momenta, etc.)
- Non-zero asymmetries are the first experimental observation of possible spin-orbit correlations between hadrons produced simultaneously in the CFR and TFR.



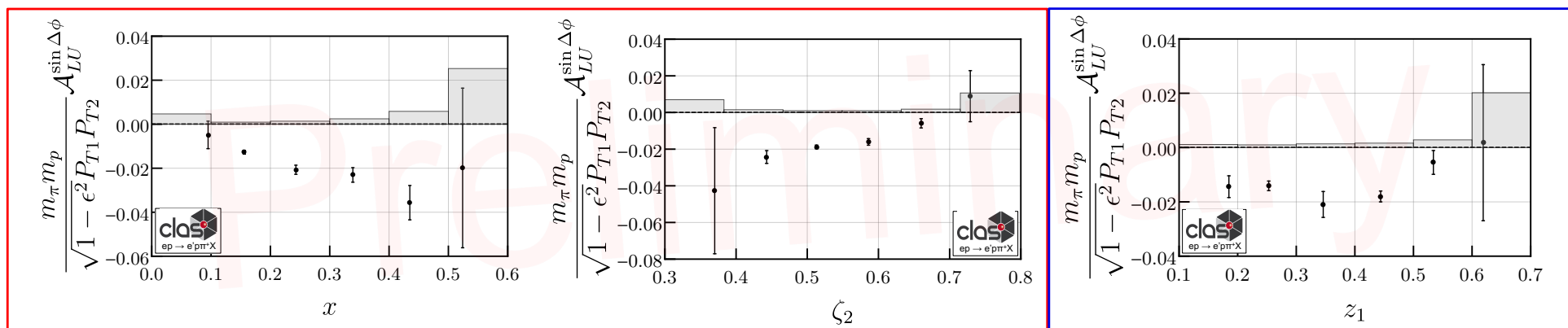
$$\mathcal{A}_{LU} = -\sqrt{1 - \epsilon^2} \frac{|\vec{P}_{T1}| |\vec{P}_{T2}|}{m_N m_2} \frac{\mathcal{C}[w_5 \hat{l}_1^{\perp h} D_1]}{\mathcal{C}[\hat{u}_1 D_1]} \sin \Delta \phi$$

Divide out the kinematic factors for clearer description of fracture and fragmentation function dependence...

Access to unmeasured fracture functions

- x-dependence increases in magnitude in the valance quark region.
- ζ_2 -dependence shows decreasing amplitude with increasing momenta. Possibly due to correlations with x.
- Relatively flat as a function of z_1 , likely due to cancellation of fragmentation functions.

$$A_{LU} \propto \frac{\mathcal{C} \left[w_5 \hat{l}_1^{\perp h}(x, \zeta_2, P_{T2}) D_1(z_1, P_{T1}) \right]}{\mathcal{C} \left[\hat{u}_1(x, \zeta_2, P_{T2}) D_1(z_1, P_{T1}) \right]}$$



Conclusions

- Kinematic dependencies of SSAs in back-to-back dihadron production observed **for the first time**.
- SSAs can be interpreted in a framework using FrFs, specifically the leading twist FrF $\hat{l}_1^{\perp h}$, describing the conditional probability of the target remnant forming a proton after the emission of a longitudinally polarized quark from an unpolarized proton.
- Future work: deuterium target, separate pion flavors, polarized targets ($\hat{u}_{1L}^{\perp h}$), etc.

The new beam-spin asymmetry introduced here has a definite and clear signature which can be experimentally tested, both in running experiments (JLab) and future ones (upgraded JLab and future electron-ion or electron-nucleon colliders, EIC/ENC). If experimentally observed, it would confirm the validity of the TMD factorization in high energy lepto-production for TFR events, thus opening new ways of exploring the nucleon internal structure.

M. Anselmino et al., Phys. Lett. B. 713 (2012), 317-320, [hep-ph] 1112.2604

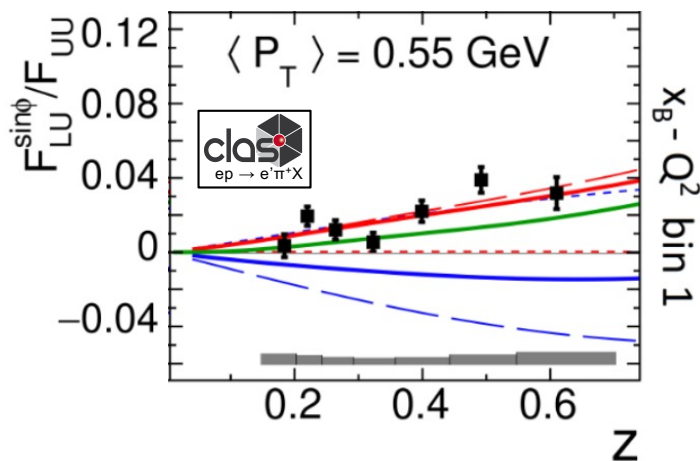


Backup Slides

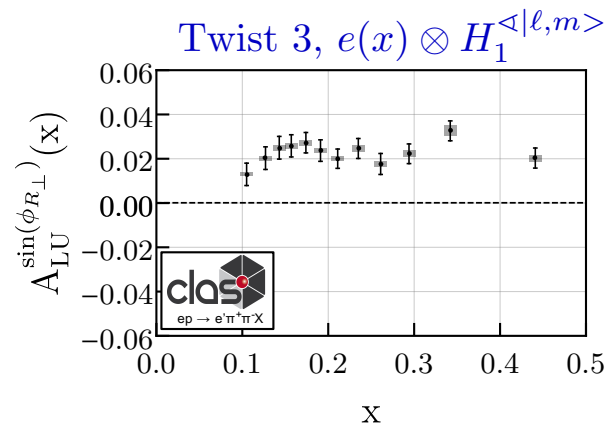
PDF Sensitive CLAS12 Measurements

- Measurements traditionally focus on factorization theorems and assumption that hadrons are produced in current fragmentation.

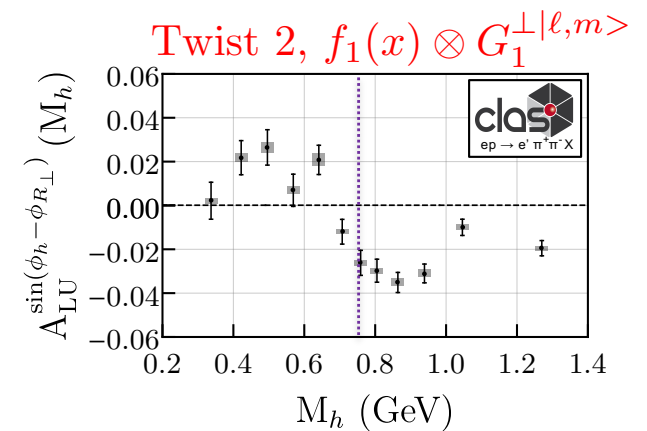
$$F_{LU}^{\sin\phi_h} = \frac{2M}{Q} C \left[-\frac{\hat{h} \cdot k_T}{M_h} \left(x e H_1^\perp + \frac{M_h}{M} f_1 \frac{\vec{G}^\perp}{z} \right) + \frac{\hat{h} \cdot p_T}{M} \left(x g^\perp D_1 + \frac{M_h}{M} h_1^\perp \frac{\vec{E}}{z} \right) \right]$$



S. Diehl et al., *Phys. Rev. Lett.*, 128, 062005, (2022), [hep:ex] 2101.03544



T. B. Hayward et al., *Phys. Rev. Lett.*, 126, 152501, (2021), [hep:ex] 2101.04842



Ambiguous Modulations

$$\frac{d\sigma^{\text{TFR}}}{dx_B dy d\zeta d^2\mathbf{P}_{h\perp} d\phi_S} = \frac{2\alpha_{\text{em}}^2}{Q^2 y} \left\{ \left(1 - y + \frac{y^2}{2}\right) \right.$$

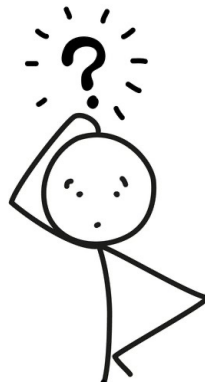
$$\times \sum_a e_a^2 \left[\hat{u}_1(x_B, \zeta, \mathbf{P}_{h\perp}^2) - |\mathbf{S}_\perp| \frac{|\mathbf{P}_{h\perp}|}{m_h} \hat{u}_{1T}^\perp(x_B, \zeta, \mathbf{P}_{h\perp}^2) \sin(\phi_h - \phi_S) \right]$$

$$+ \lambda_l y \left(1 - \frac{y}{2}\right) \sum_a e_a^2 \left[S_\parallel \hat{l}_{1L}(x_B, \zeta, \mathbf{P}_{h\perp}^2) \right.$$

$$\left. + |\mathbf{S}_\perp| \frac{|\mathbf{P}_{h\perp}|}{m_h} \hat{l}_{1T}^\perp(x_B, \zeta, \mathbf{P}_{h\perp}^2) \cos(\phi_h - \phi_S) \right] \left. \right\}.$$

M. Anselmino et al., Phys. Lett. B. 699 (2011), 108-118, [hep-ph] 1102.4214

The same azimuthal asymmetries can appear in both the CFR and TFR complicating their interpretation...



$$\left[F_{UT,T}^{\sin(\phi_h - \phi_S)} \right]_{\text{TFR}} = - \sum_a e_a^2 x_B \frac{|\mathbf{P}_{h\perp}|}{m_h} \hat{u}_{1T}^\perp(x_B, \zeta, \mathbf{P}_{h\perp}^2)$$

$$\left[F_{UT,T}^{\sin(\phi_h - \phi_S)} \right]_{\text{CFR}} = \mathcal{C} \left[- \frac{\hat{\mathbf{h}} \cdot \mathbf{k}_\perp}{m_N} f_{1T}^\perp D_1 \right]$$

$$\left[F_{LT}^{\cos(\phi_h - \phi_S)} \right]_{\text{TFR}} = \sum_a e_a^2 x_B \frac{|\mathbf{P}_{h\perp}|}{m_h} \hat{l}_{1T}^\perp(x_B, \zeta, \mathbf{P}_{h\perp}^2)$$

$$\left[F_{LT}^{\cos(\phi_h - \phi_S)} \right]_{\text{CFR}} = \mathcal{C} \left[\frac{\hat{\mathbf{h}} \cdot \mathbf{k}_\perp}{m_N} g_{1T} D_1 \right]$$

... six more azimuthal asymmetries appear in the CFR at leading twist which are absent in the TFR.

Accessing longitudinal polarization

- TFR studies provide unique access to longitudinally polarized quarks in unpolarized nucleons and unpolarized quarks in longitudinally polarized nucleons which ordinarily disappear after integration over either momentum.

		Quark polarization		
		U	L	T
Nucleon polarization	U	f_1	☹	h_1^\perp
	L	☹	g_{1L}	h_{1L}^\perp
	T	f_{1T}^\perp	g_{1T}	h_1, h_{1T}^\perp

		Quark polarization		
		U	L	T
Nucleon polarization	U	\hat{u}_1	$\hat{l}_1^{\perp h}$	$\hat{t}_1^h, \hat{t}_1^\perp$
	L	$\hat{u}_{1L}^{\perp h}$	\hat{l}_{1L}	$\hat{t}_{1L}^h, \hat{t}_{1L}^\perp$
	T	$\hat{u}_{1T}^h, \hat{u}_{1T}^\perp$	$\hat{l}_{1T}^h, \hat{l}_{1T}^\perp$	$\hat{t}_{1T}^h, \hat{t}_{1T}^{\perp h}$ $\hat{t}_{1T}^{\perp\perp}, \hat{t}_{1T}^{\perp h}$

M. Anselmino et al., Phys. Lett. B. 706 (2011), 46-52, [hep-ph] 1109.1132

Differential Cross Section

Contracting the hadronic tensor (8) with the leptonic tensor we get the differential cross section (for details of the calculations, see [13, 16]):

$$\begin{aligned}
 & \frac{d\sigma^{l(\lambda_l) N \rightarrow l h_1 h_2 X}}{dx_B dy dz_1 d\zeta_2 d\mathbf{P}_{1\perp}^2 d\mathbf{P}_{2\perp}^2 d\phi_1 d\phi_2} \\
 &= \frac{\pi\alpha_{\text{em}}^2}{x_B y Q^2} \left\{ \left(1 - y + \frac{y^2}{2}\right) \mathcal{F}_{UU} \right. \\
 &+ (1 - y) \mathcal{F}_{UU}^{\cos(\phi_1 + \phi_2)} \cos(\phi_1 + \phi_2) \\
 &+ (1 - y) \mathcal{F}_{UU}^{\cos(2\phi_1)} \cos(2\phi_1) \\
 &+ (1 - y) \mathcal{F}_{UU}^{\cos(2\phi_2)} \cos(2\phi_2) \\
 &- \lambda_l y \left(1 - \frac{y}{2}\right) \mathcal{F}_{LU}^{\sin(\phi_1 - \phi_2)} \sin \Delta\phi \left. \right\} \\
 &\equiv \sigma_{UU} + \lambda_l \sigma_{LU}, \tag{9}
 \end{aligned}$$

where λ_l is the lepton helicity and the structure functions $\mathcal{F}(x_B, z_1, \zeta_2, \mathbf{P}_{1\perp}^2, \mathbf{P}_{2\perp}^2, \mathbf{P}_{1\perp} \cdot \mathbf{P}_{2\perp})$ are given, at leading twist, by:

$$\mathcal{F}_{UU} = \mathcal{C} [\hat{u}_1 D_1], \tag{10}$$

$$\mathcal{F}_{UU}^{\cos(\phi_1 + \phi_2)} = \frac{|\mathbf{P}_{1\perp}| |\mathbf{P}_{2\perp}|}{m_1 m_2} \mathcal{C} [w_1 \hat{t}_1^h H_1^\perp] \tag{11}$$

$$\mathcal{F}_{UU}^{\cos(2\phi_1)} = \frac{\mathbf{P}_{1\perp}^2}{m_1 m_N} \mathcal{C} [w_2 \hat{t}_1^\perp H_1^\perp] \tag{12}$$

$$\begin{aligned}
 \mathcal{F}_{UU}^{\cos(2\phi_2)} &= \frac{\mathbf{P}_{2\perp}^2}{m_1 m_2} \mathcal{C} [w_3 \hat{t}_1^h H_1^\perp] \\
 &+ \frac{\mathbf{P}_{2\perp}^2}{m_1 m_N} \mathcal{C} [w_4 \hat{t}_1^\perp H_1^\perp] \tag{13}
 \end{aligned}$$

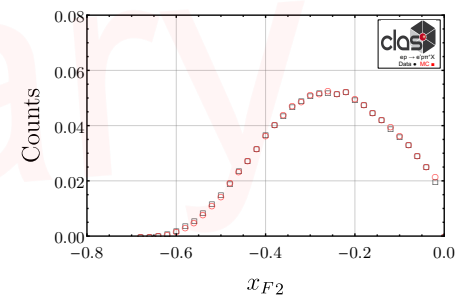
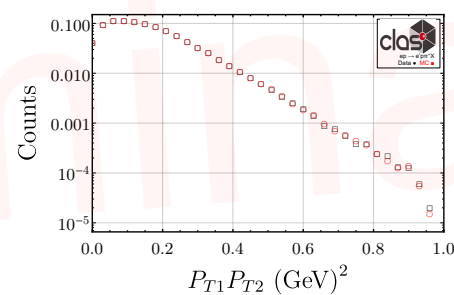
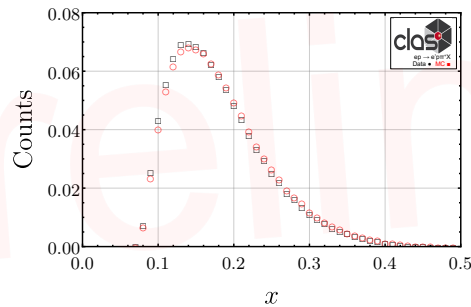
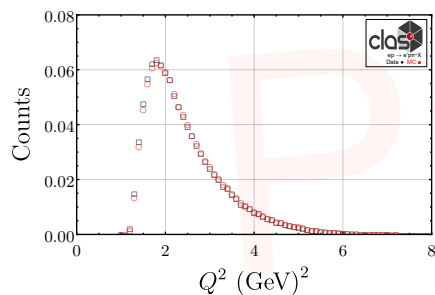
$$\mathcal{F}_{LU}^{\sin(\phi_1 - \phi_2)} = \frac{|\mathbf{P}_{1\perp}| |\mathbf{P}_{2\perp}|}{m_N m_2} \mathcal{C} [w_5 \hat{t}_1^{\perp h} D_1], \tag{14}$$

with the following notation for the transverse momentum convolution

$$\begin{aligned}
 \mathcal{C} [f(\mathbf{k}_\perp, \mathbf{k}'_\perp, \dots)] &\equiv \sum_a e_a^2 x_B \int d^2\mathbf{k}_\perp \int d^2\mathbf{k}'_\perp \\
 &\times \delta^2(\mathbf{k}_\perp - \mathbf{k}'_\perp - \mathbf{P}_{1\perp}/z_1) f(\mathbf{k}_\perp, \mathbf{k}'_\perp, \dots). \tag{15}
 \end{aligned}$$

Monte Carlo

- SIDIS MC “clasdis”¹ based on PEPSI² generator, the polarized version of the well-known LEPTO³ generator.
- Parameters changed to reproduce observed distributions include average transverse momentum, fraction of spin-1 light mesons and fraction of spin-1 strange mesons.
- CLAS12 detector system described in “GEMC”⁴, a detailed GEANT4 simulation package.
- Excellent agreement between data and MC!

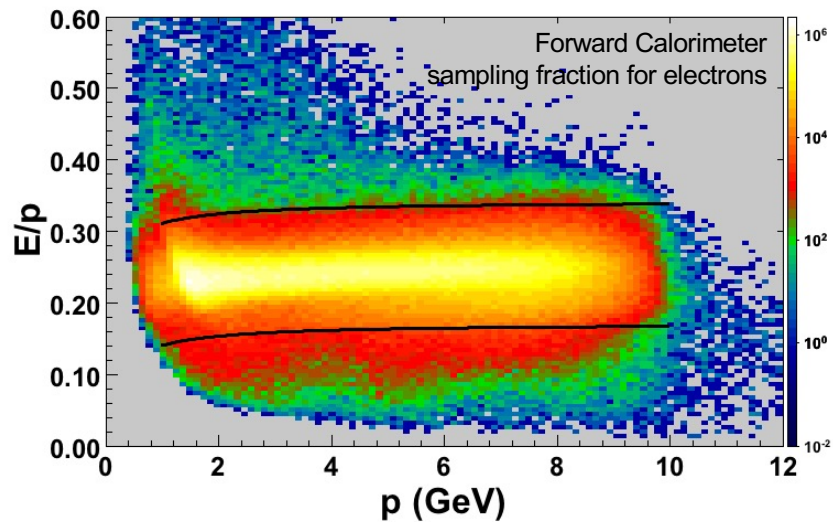


1. H. Avakian, “clasdis.” <https://github.com/JeffersonLab/clasdis>, 2020.
2. L. Mankiewicz, A. Schafer, and M. Veltri, “Pepsi: A monte carlo generator for polarized leptoproduction,” *Comput. Phys. Commun.*, vol. 71, pp. 305–318, 1992.
3. G. Ingelman, A. Edin, and J. Rathsmann, “LEPTO 6.5: A Monte Carlo generator for deep inelastic lepton - nucleon scattering,” *Comput. Phys. Commun.*, vol. 101, pp. 108–134, 1997.
4. M. Ungaro et al., “The CLAS12 Geant4 simulation,” *Nucl. Instrum. Meth. A*, vol. 959, p. 163422, 2020.

Particle ID

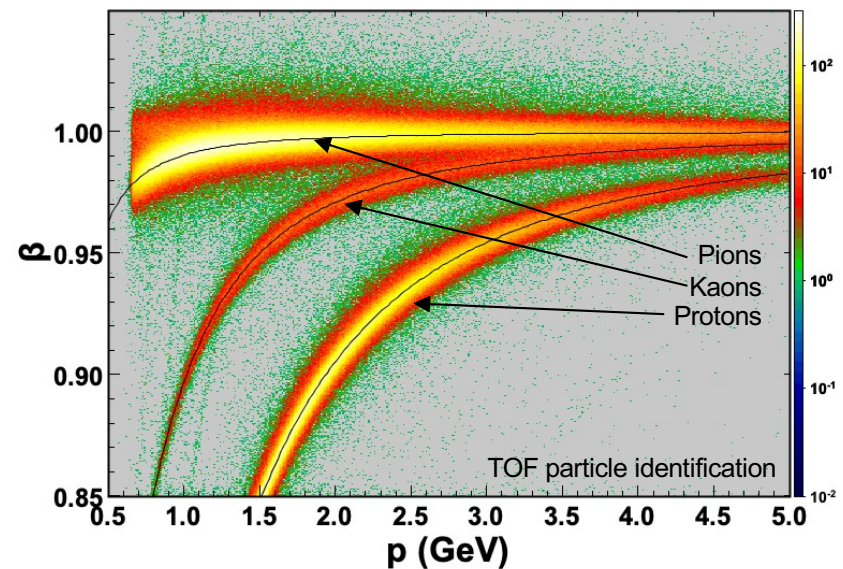
- Electron

- Electromagnetic calorimeter.
- Cherenkov detector.
- Vertex and fiducial cuts.

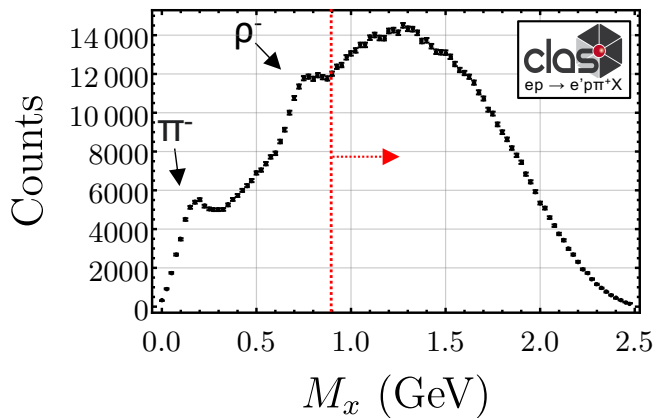


- Hadron

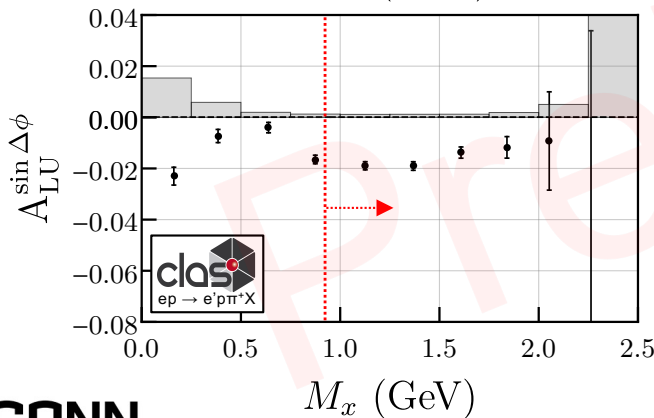
- β vs p comparison between vertex timing and event start time.
- Vertex and fiducial cuts.
- Pion momentum limited to < 4 GeV.



Removing background

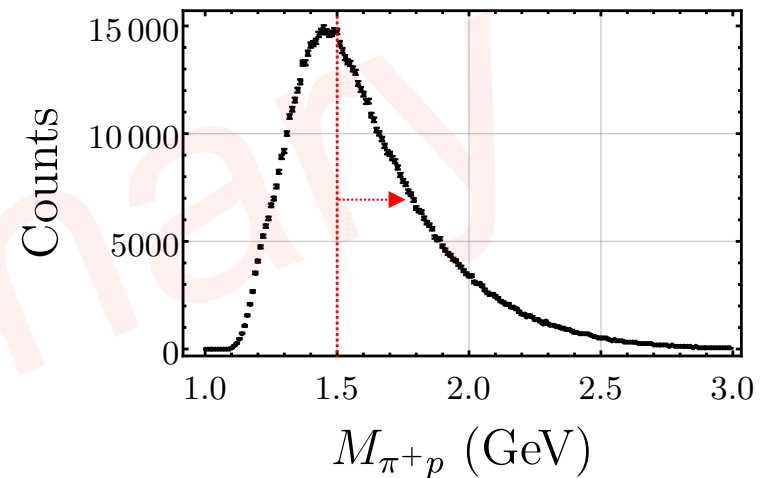


- Exclusive pion and rho production clearly visible.



- Different amplitudes at low M_x are generated from separate physics than our signal.

$\Delta^{++} \rightarrow p\pi^+$ Contamination?



- Little sign of Δs ; cut on mass > 1.5 GeV for safety.
- Estimate remaining contribution from MC.

Additional Modulations

$$\mathcal{F}_{LU} = \frac{|p_{\pi}^{\perp}| |p_{P}^{\perp}|}{m_p m_{\pi}} \mathcal{C} \left[w_5 \hat{l}_1^{\perp h} D_1 \right] \longrightarrow$$

Phys. Lett. B. 713 (2012), 317-320, [hep-ph] 1112.2604

Structure functions carry a dependence on $|p_{\pi}^{\perp}| |p_{P}^{\perp}|$ which introduces a dependence on $\cos \Delta\phi$.

If the correlations are assumed small, the fracture functions can be expanded in powers of $k^{\perp} \cdot p_{P}^{\perp}$.

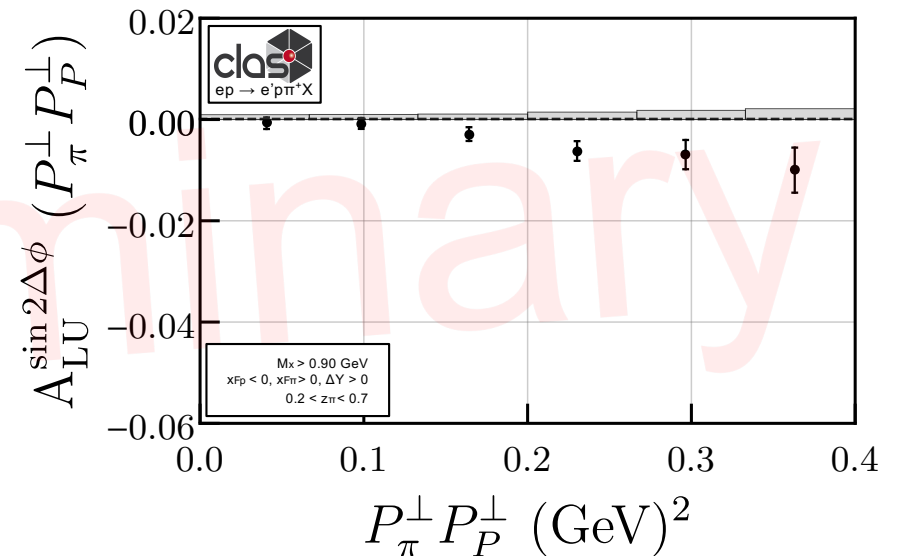
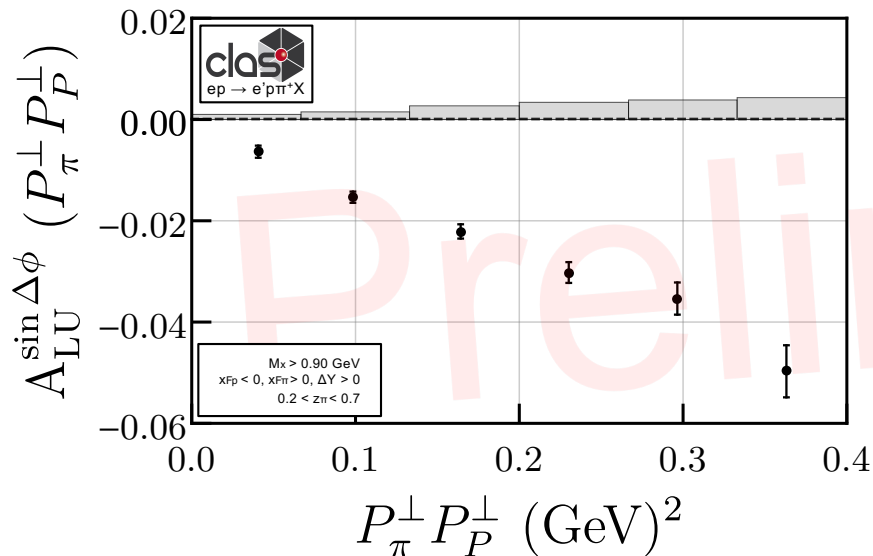
$$\begin{aligned} \hat{l}_1^{\perp h}(x, \zeta, \mathbf{k}^{\perp 2}, \mathbf{p}_{P}^{\perp 2}, \mathbf{k}^{\perp} \cdot \mathbf{p}_{P}^{\perp}) \\ \approx a(x, \zeta, \mathbf{k}^{\perp 2}, \mathbf{p}_{P}^{\perp 2}) \\ + b(x, \zeta, \mathbf{k}^{\perp 2}, \mathbf{p}_{P}^{\perp 2}) \mathbf{k}^{\perp} \cdot \mathbf{p}_{P}^{\perp} \end{aligned}$$

The term linear in $k^{\perp} \cdot p_{P}^{\perp}$ yields a $\cos \Delta\phi$ which when combined with the already existing $\sin \Delta\phi$ term results in a $\sin 2\Delta\phi$.

$$\mathcal{A}_{LU}(x, \zeta, \mathbf{k}^{\perp 2}, \mathbf{p}_{P}^{\perp 2}, \Delta\phi) = A(x, \zeta, \mathbf{k}^{\perp 2}, \mathbf{p}_{P}^{\perp 2}) \sin \Delta\phi + B(x, \zeta, \mathbf{k}^{\perp 2}, \mathbf{p}_{P}^{\perp 2}) \sin(2\Delta\phi)$$

Additional modulation is small

- The $\sin(2\Delta\phi)$ is mostly (coincidentally) very small.
- Still important to extract simultaneously.



Directly plotting FrFs and FFs

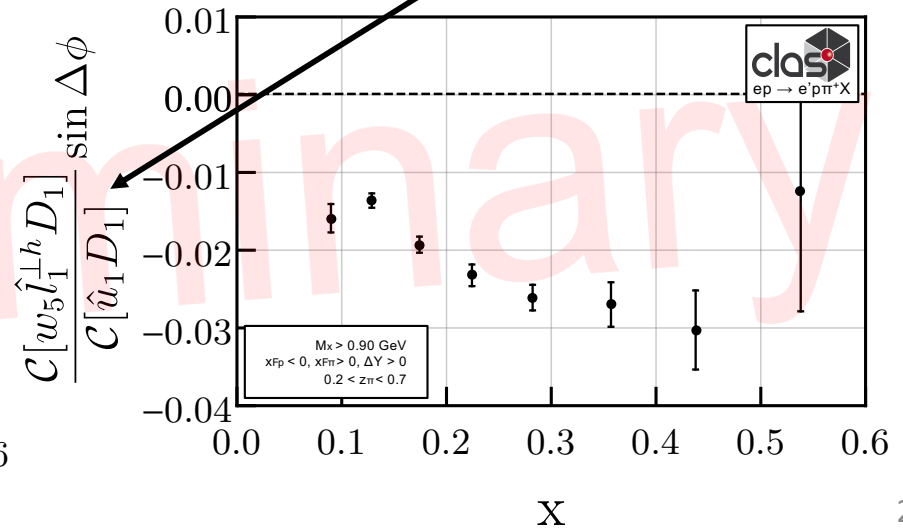
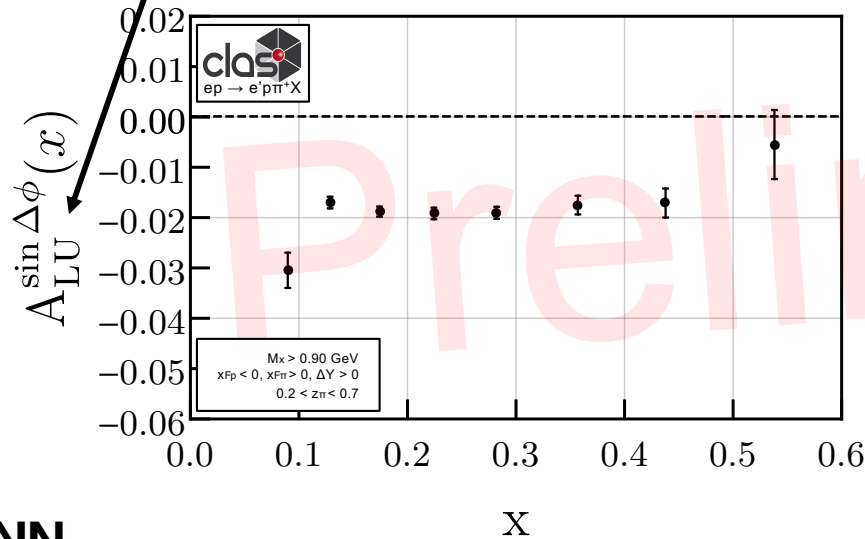
Depolarization Structure Functions

$$A_{LU}^{\sin \Delta\phi} = - \frac{1 - \frac{y}{2}}{1 - y + \frac{y^2}{2}} \frac{\mathcal{F}_{LU}^{\sin \Delta\phi}}{\mathcal{F}_{UU}} \sin \Delta\phi,$$

Depolarization

Structure Functions

$$= - \frac{y \left(1 - \frac{y}{2}\right)}{\left(1 - y + \frac{y^2}{2}\right)} \frac{|\mathbf{P}_{1\perp}| |\mathbf{P}_{2\perp}| \mathcal{C}[w_5 \hat{l}_1^{\perp h} D_1]}{m_N m_2 \mathcal{C}[\hat{u}_1 D_1]} \sin \Delta\phi.$$



Subtly different z definitions

In the TFR the factorization in x_B and z_h of Eq. (3) does not hold any longer, as it is not possible to separate the quark emission from the hadron production. Moreover, z_h is not the proper variable to describe this region. The reason is easily understood if we write z_h in the c.m. γ^*N frame (we neglect as usual hadron masses):

$$z_h = \frac{E_h}{E(1-x_B)} \frac{(1-\cos\theta_h)}{2}, \quad (4)$$

where θ_h is the angle between \mathbf{P}_h and \mathbf{P} . The z_h variable does not discriminate between two different physical situations, namely $E_h = 0$ (soft hadron emission) and $\theta_h = 0$ (target fragmentation: emission of a hadron collinear with the target remnant), which both correspond to $z_h = 0$.

In order to describe the production of hadrons in the target fragmentation region, one has to define the fracture functions $M_a(x_B, (1-x_B)z)$, which depend on x_B and on a new variable $z = E_h/E(1-x_B)$, and represent the distributions of partons inside a nucleon fragmenting almost collinearly into a given hadron [4, 5]. Notice that, differently from z_h , the variable z vanishes in the soft limit only ($E_h \rightarrow 0$). The SIDIS cross section in the TFR, integrated over the transverse momentum of the final hadron, thus becomes

$$\frac{d\sigma^{\text{TFR}}}{dx_B dy dz} = \sum_a e_a^2 (1-x_B) M_a(x_B, (1-x_B)z) \frac{d\hat{\sigma}}{dy}. \quad (5)$$

M. Anselmino et al., Phys. Lett. B. 706 (2011), 46-52, [hep-ph] 1109.1132

Fracture Functions Renamed

Leading Twist

	U	L	T
U	M	$M_L^{\perp,h}$	M_T^h, M_T^\perp
L	$\Delta M^{\perp,h}$	ΔM_L	$\Delta M_T^h, \Delta M_T^\perp$
T	$\Delta_T M_T^h, \Delta_T M_T^\perp$	$\Delta_T M_L^h$ $\Delta_T M_L^\perp$	$\Delta_T M_T, \Delta_T M_T^{hh}$ $\Delta_T M_T^{\perp\perp}, \Delta_T M_T^{\perp h}$

Quark polarization

	U	L	T
U	\hat{u}_1	$\hat{l}_1^{\perp h}$	$\hat{t}_1^h, \hat{t}_1^\perp$
L	$\hat{u}_{1L}^{\perp h}$	\hat{l}_{1L}	$\hat{t}_{1L}^h, \hat{t}_{1L}^\perp$
T	$\hat{u}_{1T}^h, \hat{u}_{1T}^\perp$	$\hat{l}_{1T}^h, \hat{l}_{1T}^\perp$	$\hat{t}_{1T}, \hat{t}_{1T}^{hh}$ $\hat{t}_{1T}^{\perp\perp}, \hat{t}_{1T}^{\perp h}$

ALU(xF_p)

